



Chebyshev Collocation Method for the Effect of Variable Thermal Conductivity on Micropolar Fluid Flow over Vertical Cylinder with Variable Surface Temperature

Nasser S. Elgazery¹
Nader Y. Abd Elazem²
Department of Mathematics
Ain Shams University
Roxy, Heliopolis, Cairo, Egypt

Received: June 14, 2007; Accepted: October 20, 2007

Abstract

An analysis is performed to study the role of a variable thermal conductivity on unsteady free-convection in a micro-polar fluid past a semi-infinite vertical cylinder with variable surface temperature in the presence of magnetic field and radiation. The surface temperature is measured to vary as a power of the axial coordinate measured from the leading edge of the cylinder. The governing non-linear partial differential equations are transformed into a linear algebraic system utilizing Chebyshev collocation method in spatial and Crank-Nicolson method in time. Numerical results for the velocity, angular velocity and temperature profiles as well as for the local skin friction, couple stress and Nusselt number are obtained and reported in tabular form and graphically for various parametric conditions to show interesting aspects of the solution. The velocity and temperature profiles are compared with the available results in the literature and it is found to be in good agreement.

Keyword: Chebyshev Collocation Method, Micropolar Fluid, Variable Thermal Conductivity, Vertical Cylinder, Variable Surface Temperature

AMS 2000 Subject Classification Numbers: 65N06, 76S05, 76D05

1. Introduction

Because of the increasing importance of materials flow in industrial processing and elsewhere, and the fact that shear behavior can not be characterized by Newtonian relationships, a new stage in the evaluation of fluid-dynamic theory is in progress. The theory of micro-polar fluids which

¹Present address Preparatory Year Unit, Al-Qassim University, P.O. Box 6595, Al-Qassim, Buraidah: 51452 Saudi Arabia,
E-mail address: nasser_522000@yahoo.com

²E-mail address: naderelnafrawy@yahoo.com

displays the effects of local rotary inertia and couple stresses was formulated by Eringen (1966). The theory can be used to explain the flow of colloidal fluids, liquid crystals, animal blood etc. Eringen (1972) extended the micro-polar fluid theory and developed the theory of thermomicro-polar fluids. The study of micro-polar fluid flows with heat transfer has important engineering applications, for example, in power generators, refrigeration coils, transmission lines, electric transformers and heating elements.

The most common type of body force, which acts on a fluid, is due to gravity, so that the body force can be defined as in magnitude and direction by the acceleration due to gravity. Sometimes, electromagnetic effects are important. The electric and magnetic fields themselves must obey a set of physical laws, which are expressed by Maxwell's equations. The solution to such problems requires the simultaneous solution of the equations of fluid mechanics and of electromagnetism. One special case of this type of coupling is the field known as magnetohydrodynamic (MHD). The effect of radiation on MHD flow and heat transfer problems has become industrially more important.

Many engineering processes occur at high temperatures and the knowledge of radiation heat transfer has become very important for the design of pertinent equipment. Nuclear power plants, gas turbines and various propulsion devices for aircraft, missiles, satellites and space vehicles are examples of such engineering processes, i.e., at high operating temperature, radiation effect can be quite significant. Dring and Gebhart (1966) presented transient natural convection from thin vertical cylinders. Lee et al. (1988) studied the natural convection along slender vertical cylinders with variable surface temperature. Badr and Dennis (1985) carried out a time dependent viscous flow past an impulsively started rotating and translating circular cylinder. Collins and Dennis (1973) made a numerical extension of the method of expansion in powers of the time for an impulsively started circular cylinder by using an implicit time-dependent numerical integration procedure and symmetrical flow past a uniformly accelerated circular cylinder. Evans et al. (1980) studied transient natural convection in vertical cylinder.

Chen and Yih (1980) studied combined heat and mass transfer in natural convection along vertical cylinder. Velusamy and Garg (1992) studied transient natural convection over a heat generating vertical cylinder. Ganesan and Rani (1998) studied transient natural convection along vertical cylinder with heat and mass transfer. Ganesan et al. (2000) studied transient natural convection flow over vertical cylinder with variable surface temperature. Ganesan and Loganathan (2001a, b, c, 2002, 2003, 2006) studied the problem of unsteady flow with heat and mass transfer past a moving vertical cylinder for different cases of constant heat flux, mass flux, chemically reactive species diffusion, uniform temperature and concentration at the cylinder surface and in the presence of constant applied magnetic field normal to the surface of the cylinder.

All these studies were not concerned with unsteady free-convection in a micro-polar fluid flow past a semi-infinite vertical cylinder with variable surface temperature in the presence of magnetic field and radiation. Hence, the purpose of this work is to extend Ganesan et al. (2000), to study the more general problem, which includes variable thermal conductivity effect on MHD unsteady free-convection in a micro-polar fluid past a semi-infinite vertical cylinder with variable surface temperature in the presence of radiation. The fluid thermal conductivity is

assumed to vary linearly with temperature. The dimensionless non-linear partial differential equations are solved numerically by using Chebyshev collocation scheme. It is hoped that the results obtained will not only provide useful information for applications but also serve as a complement to the previous studies.

2. Mathematical formulation

Unsteady flow of an electrically conducting viscous micro-polar fluid past a semi-infinite vertical cylinder of radius r_0 with variable surface temperature is considered. The x -axis is measured vertically upward along the axis of the cylinder. The radial coordinate r -axis is measured normal to axis of the cylinder. A uniform magnetic field of strength β_0 is imposed along the r -axis (see Fig. 1).

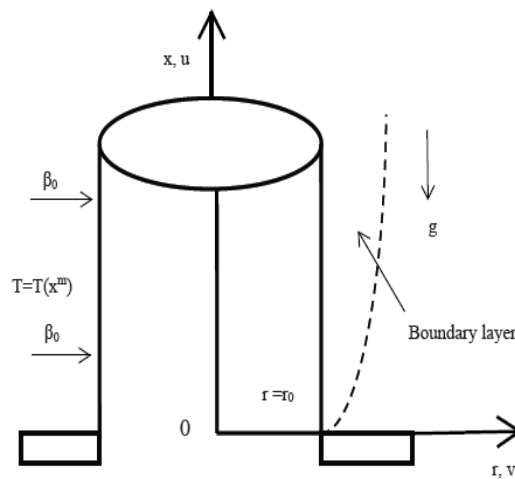


Fig.1 Sketch of the physical model

Initially, at time $\tilde{t} = 0$, it is assumed that a vertical cylinder and the fluid are at the same temperature T_∞ . At time $\tilde{t} \geq 0$, the cylinder temperature is assumed to vary as the power of the axial coordinate. It is also assumed that the fluid properties are isotropic and constant, except for the fluid thermal conductivity, k_f , which is assumed to vary as a linear function of temperature, T , in the form (Schlichting (1972)) $k_f = k_\infty(1 + a(T - T_\infty))$, where k_f , T and T_∞ are the fluid free-stream thermal conductivity, the temperature of the fluid in the boundary layer and the fluid free-stream temperature. a is a constant depending on the nature of the fluid, in general, $a > 0$ for fluids such as water and air, while $a < 0$ for fluids such as lubrication oils. This form can be rewritten in the form $k_f = k_\infty(1 + S\theta)$, where $S = a(T_w - T_\infty)$, is the thermal conductivity parameter and T_w is the average value of the plate temperature of the fluid in the boundary layer. The range of variation of S can be taken as follows (see Schlichting (1972)) (for air $0 \leq S \leq 6$, for water $0 \leq S \leq 0.12$ and for lubrication oils $-0.1 \leq S \leq 0$). The radiating gas is said to be a non-gray if the absorption coefficient k_λ is dependent on the wavelength λ . The equation which describes the conservation of radiative transfer in a unit volume (includes the radiative energy incident from all directions) is given for all wavelength as

$$\nabla \cdot \underline{q}_r = \int_0^\infty K_\lambda(T) (4e_{\lambda h}(T) - G_\lambda) d\lambda,$$

where $e_{\lambda h}$ is the Planck's function and the incident radiation G_λ is defined as

$$G_\lambda = \frac{1}{\pi} \int_{\Omega=4\pi} e_\lambda(\Omega) d\Omega,$$

where $\nabla \cdot \underline{q}_r$ is the radiative flux divergence and Ω is the solid angle. Now, for an optically thin fluid exchanging radiation with an isothermal flat plate at temperature T_w and according to the above definition for the radiative flux divergence and Kirchhoffs law the incident radiation is given by

$$G_\lambda = 4e_{b\lambda}(T_w),$$

then,

$$\nabla \cdot \underline{q}_r = 4 \int_0^\infty K_\lambda(T) (e_{\lambda h}(T) - e_{\lambda h}(T_w)) d\lambda.$$

Expanding K_λ and $e_{\lambda h}(T_w)$ in Taylor series around T_w for small $T - T_w$, then we can rewrite the radiative flux divergence as

$$\nabla \cdot \underline{q}_r = 4(T - T_w) \int_0^\infty K_{\lambda w} \left(\frac{\partial e_{\lambda h}}{\partial T} \right)_w d\lambda,$$

where

$$K_{\lambda w} = K_\lambda(T_w).$$

Hence, an optical thin limit for a non-gray gas near equilibrium, the following relation holds (Cogley et al. (1968))

$$\frac{\partial q_r}{\partial R} = 4(T - T_w)I,$$

where,

$$I = \int_0^\infty K_{\lambda w} \left(\frac{\partial e_{\lambda h}}{\partial T} \right)_w d\lambda.$$

Under the Boussinesq and boundary layer approximations, the governing continuity, momentum, angular momentum and energy conservation equations become (Ganesan et al. (2000)):

$$\frac{\partial(ru)}{\partial x} + \frac{\partial(rv)}{\partial r} = 0, \tag{1}$$

$$\frac{\partial u}{\partial t} + u \frac{\partial u}{\partial x} + v \frac{\partial u}{\partial r} = g\beta(T - T_\infty) + \frac{v}{r} \frac{\partial}{\partial r} \left(r \frac{\partial u}{\partial r} \right) - \frac{\sigma}{\rho} \beta_0^2 u + \frac{k}{\rho} \frac{\partial G}{\partial r}, \tag{2}$$

$$\frac{\partial G}{\partial \tilde{t}} + u \frac{\partial G}{\partial x} + v \frac{\partial G}{\partial r} = \frac{\gamma}{j\rho} \frac{1}{r} \frac{\partial}{\partial r} \left(r \frac{\partial G}{\partial r} \right) + \frac{k}{j\rho} \left(\frac{\partial u}{\partial r} - \frac{\partial v}{\partial x} - 2G \right), \quad (3)$$

$$\frac{\partial T}{\partial \tilde{t}} + u \frac{\partial T}{\partial x} + v \frac{\partial T}{\partial r} = \frac{1}{\rho c_p} \frac{1}{r} \frac{\partial}{\partial r} \left(r k_f \frac{\partial T}{\partial r} \right) - 4(T - T_w)I. \quad (4)$$

Where u and v are the velocity components in the x and r directions, respectively, and G is the component of microrotation whose direction of rotation in the $(x-r)$ plane. T is the temperature of the fluid in the boundary layer, \tilde{t} is the time, g is the acceleration due to gravity, the temperature of the surface is T_w and far away from the surface this value is invariant and is represented by T_∞ . ν , ρ and β are the fluid kinematic viscosity, the density of the fluid and the volumetric coefficient of thermal expansion. \underline{q}_r , β_0 and σ are the radiation heat flux, the applied magnetic field and the electric conductivity, respectively. j , γ , k , k_f , and c_p are the microinertia per unit mass, the spin gradient viscosity, the non-Newtonian consistency index, the fluid thermal conductivity and the fluid specific heat, respectively.

The initial and boundary conditions are

$$\tilde{t} = 0: u = v = 0, T = T_\infty, G = 0, \text{ for all } x \text{ and } r$$

$$\tilde{t} > 0: \begin{cases} u = v = 0, T = T_\infty, G = 0, & \text{at } x = 0 \text{ for all } r, \\ u = 0, v = 0, G = -\frac{1}{2} \frac{\partial u}{\partial r}, \\ T = T_\infty + (T_w - T_\infty) x^m, & \text{at } x > 0 \text{ as } r = r_0, \\ u = 0, T \rightarrow T_\infty, G \rightarrow 0, & \text{at } x > 0 \text{ as } r \rightarrow \infty. \end{cases} \quad (5)$$

Knowing the following non-dimensional quantities:

$$\begin{aligned} X &= \frac{x}{r_0}, & R &= \frac{r R_0}{r_0}, & U &= \frac{u r_0}{\nu R_0^2}, & V &= \frac{v r_0}{\nu R_0}, & t &= \frac{\nu R_0^2}{r_0^2} \tilde{t}, \\ \theta &= \frac{T - T_\infty}{T_w - T_\infty}, & Gr_0 &= \frac{g \beta (T_w(r_0) - T_\infty) r_0^3}{\nu^2}, & R_0 &= Gr_0^{\frac{1}{4}}, \\ F &= \frac{4 I r_0^2}{\nu R_0^2}, & Pr &= \frac{\nu \rho c_p}{k_\infty}, & M &= \frac{\sigma \beta_0^2 r_0^2}{\mu R_0^2} \end{aligned} \quad (6)$$

Gr_0 is the Grashof number, Pr is the Prandtl number, M is the magnetic parameter, F is the radiation parameter and μ is the viscosity coefficient.

We introduce the following dimensionless variable of the angular velocity and parameters of micropolar and material of fluid (Cheng and Huann (1994))

$$G = \frac{\mu Gr_0^{\frac{3}{4}}}{\rho r_0^2} g, R^* = \frac{k}{\mu}, B = \frac{r_0^2}{jGr_0^{\frac{1}{2}}}, \lambda = \frac{\gamma}{\mu j}, \tag{7}$$

where, R^* is the micropolar parameter, B and λ are materials parameters.

We can obtain the governing equations in dimensionless form:

$$\frac{\partial(RU)}{\partial X} + \frac{\partial(RV)}{\partial R} = 0, \tag{8}$$

$$\frac{\partial U}{\partial t} + U \frac{\partial U}{\partial X} + V \frac{\partial U}{\partial R} = \theta + \frac{1}{R} \frac{\partial}{\partial R} \left(R \frac{\partial U}{\partial R} \right) - MU + R^* \frac{\partial g}{\partial R}, \tag{9}$$

$$\frac{\partial g}{\partial t} + U \frac{\partial g}{\partial X} + V \frac{\partial g}{\partial R} = \frac{\lambda}{R} \frac{\partial}{\partial R} \left(R \frac{\partial g}{\partial R} \right) + R^* B \left(\frac{\partial U}{\partial R} - \frac{1}{R^2} \frac{\partial V}{\partial X} - 2g \right), \tag{10}$$

$$\frac{\partial \theta}{\partial t} + U \frac{\partial \theta}{\partial X} + V \frac{\partial \theta}{\partial R} = \frac{(1+S\theta)}{\text{Pr}} \frac{1}{R} \frac{\partial}{\partial R} \left(R \frac{\partial \theta}{\partial R} \right) + \frac{S}{\text{Pr}} \left(\frac{\partial \theta}{\partial R} \right)^2 - F(\theta - 1). \tag{11}$$

The initial and boundary conditions are now given

$$t = 0: U = V = \theta = g = 0, \text{ for all } X \text{ and } R$$

$$t > 0: \begin{cases} U = V = \theta = g = 0, & \text{at } X = 0 \text{ for all } R, \\ U = 0, V = 0, \theta = X^m, \\ g = -\frac{1}{2} \frac{\partial U}{\partial R}, & \text{at } X > 0 \text{ as } R = R_0, \\ U = 0, \theta \rightarrow 0, g \rightarrow 0, & \text{at } X > 0 \text{ as } R \rightarrow \infty. \end{cases} \tag{12}$$

3. Skin Friction, Couple Stress and Nusselt Number

The local skin friction factor is given by

$$C_f = \frac{2\tau_w}{\rho \hat{U}}, \tag{13}$$

where, the wall shear stress may be written as

$$\tau_w = \left((\mu + k) \frac{\partial u}{\partial r} + kG \right)_{r=r_0}, \tag{14}$$

and

$$\hat{U} = \frac{\mu Gr_0^{\frac{1}{2}}}{\rho r_0},$$

is the characteristic velocity. In terms of the non-dimensional quantities, we have

$$C_f = \left(\frac{1}{Gr_0} \right)^{\frac{1}{4}} (2 + R^*) \left(\frac{\partial U}{\partial R} \right)_{R=R_0}. \quad (15)$$

The dimensionless wall couple stress coefficient is giving by

$$M_w = \left(\frac{1}{Gr_0} \right)^{\frac{1}{2}} \frac{\lambda}{B} \left(\frac{\partial g}{\partial R} \right)_{R=R_0}. \quad (16)$$

Finally, the local Nusselt number is giving by

$$N_u = - \left(\frac{1}{Gr_0} \right)^{\frac{1}{4}} \left(\frac{\partial \theta}{\partial R} \right)_{R=R_0}. \quad (17)$$

Table (1): the effects of the parameter R^* , S , F , M and m on C_f , N_u and M_w at $x = 1$, $Pr = 0.7$, $B = 0.0001$, $\lambda = 0.001$ and $t = 4.5$ (steady state)

R^*	S	F	M	m	C_f	N_u	M_w
3	0.5	0.01	10	0.2	-0.02093885	0.32373270	0.03119453
3.5					-0.02813669	0.32622709	0.00408195
4					-0.2900894	0.32664124	0.00100512
5					-0.02916221	0.32708868	-0.000912892
5	0	0.01	10	0.2	-0.02520876	0.28400323	-0.00032548
	0.5				-0.02916221	0.32708868	-0.00091289
	1.0				-0.03245033	0.36168925	-0.00145325
	2.0				-0.03742057	0.40920710	-0.00227851
5	0.5	0.01	10	0.2	-0.02916221	0.03270886	-0.00091289
		0.06			-0.03122853	0.34880765	-0.00135533
		0.1			-0.03285530	0.36544803	-0.00168535
		0.5			-0.04769786	0.50318258	-0.00364650
5	0.5	0.01	0	0.2	-0.22213301	0.28955188	-0.01174184
			3		-0.08612556	0.31692594	-0.00550343
			5		-0.05665713	0.32198716	-0.00323339
			10		-0.02916221	0.32708868	-0.00091289
5	0.5	0.01	10	0	-0.03552461	0.38730649	-0.00389076
				0.2	-0.02916221	0.32708868	-0.00091289
				0.5	-0.02296963	0.25622420	0.0008322
				1.0	-0.01617056	0.17502766	0.0014140

4. Chebyshev Collocation Method

A numerical solution based on Chebyshev collocation approximations seems to be a very good choice in many practical problems. Recently, Elgazery (2008) explain that this method is given excellent result in this kind of problems. So, we shall present Chebyshev collocation method for our model problem because of the domain has a rectangular shape. The Chebyshev collocation method is used in spatial and the time derivatives are computed with Crank-Nicolson method. The derivatives of the function $f(x)$ at the Gauss-Lobatto points, $x_k = \cos\left(\frac{k\pi}{L}\right)$, which are the linear combination of the values of the function $f(x)$ (Elbarbary and El-Sayed (2005)):

$$f^{(n)} = D^{(n)} f,$$

where

$$\underline{f} = [f(x_0), f(x_1), \dots, f(x_L)]^T,$$

and

$$\underline{f}^{(n)} = [f^{(n)}(x_0), f^{(n)}(x_1), \dots, f^{(n)}(x_L)]^T,$$

where

$$D^{(n)} = [d_{k,j}^{(n)}],$$

or

$$f^{(n)}(x_k) = \sum_{j=0}^L d_{k,j}^{(n)} f(x_j),$$

where

$$d_{k,j}^{(n)} = \frac{2\gamma_j^*}{L} \sum_{l=n}^L \sum_{\substack{m=0 \\ (m+l-n)\text{ even}}}^{l-n} \gamma_l^* a_{m,l}^n (-1)^{\lfloor \frac{l-j}{L} \rfloor + \lfloor \frac{mk}{L} \rfloor} x_{l-j-L\lfloor \frac{l-j}{L} \rfloor} x_{mk-L\lfloor \frac{mk}{L} \rfloor},$$

where

$$a_{m,l}^n = \frac{2^n l}{(n-1)! c_m} \frac{(s-m+n-1)!(s+n-1)!}{(s)!(s-m)!},$$

such that $2s = l + m - n$ and $c_0 = 2, c_i = 1, i \geq 1$, where $k, j = 0, 1, 2, \dots, L$ and $\gamma_0^* = \gamma_l^* = \frac{1}{2}, \gamma_j^* = 1$ for $j = 1, 2, 3, \dots, L-1$. The round off errors incurred during computing differentiation matrices $D^{(n)}$ are investigated in (Elbarbary and El-Sayed (2005)).

5. Descriptions of the Method for the Governing Equations

In this section the non-linear partial differential equations (8)-(11), with initial and boundary conditions (12) are approximated by using Chebyshev collocation method (Elbarbary and El-Sayed (2005) and Elbarbary and El-Kady (2003)). In the time direction, the derivatives are replaced by implicit finite-difference approximations, whereas in spatial, the derivatives are replaced by Chebyshev collocation method. Let Δt be the step sizes in time direction. The grid points (x_i, x_j, t_k) in this situation are given as $x_i = \cos\left(\frac{i\pi}{L_1}\right), x_j = \cos\left(\frac{j\pi}{L_2}\right)$, for $i = 1, \dots, L_1 - 1, j = 1, \dots, L_2 - 1$ and $t_k = \Delta t k, k = 0, 1, 2, \dots$. The domain in the X -direction is $[0, X_{\max}]$ where X_{\max} is the length of the dimensionless axial coordinate and the domain in the R -direction is $[0, R_{\max}]$ where R_{\max} corresponds to R_∞ which lies very well outside both the momentum and energy boundary layers. The domain $[0, X_{\max}] \times [0, R_{\max}]$ is mapped into the computational domain $[-1, 1] \times [-1, 1]$ and the equations (8)-(11) are transformed into the following equations:

$$\left(\frac{1}{X_{\max}}\right)\frac{\partial}{\partial X}(U_{i,j}^{k+1} + U_{i,j}^k) + \left(\frac{1}{R_{\max} - R_0}\right)\frac{\partial}{\partial R}(V_{i,j}^{k+1} + V_{i,j}^k) + \frac{V_{i,j}^{k+1}}{R} = 0, \tag{18}$$

$$\begin{aligned} & \frac{(U_{i,j}^{k+1} - U_{i,j}^k)}{\Delta t} + \left(\frac{U_{i,j}^k}{X_{\max}}\right)\frac{\partial}{\partial X}(U_{i,j}^{k+1} + U_{i,j}^k) + \left(\frac{V_{i,j}^k}{R_{\max} - R_0}\right)\frac{\partial}{\partial R}(U_{i,j}^{k+1} + U_{i,j}^k) \\ &= \left(\frac{1}{R_{\max} - R_0}\right)\left(\frac{2}{R_{\max} - R_0}\frac{\partial^2}{\partial R^2}(U_{i,j}^{k+1} + U_{i,j}^k) + \frac{1}{\bar{R}}\frac{\partial}{\partial R}(U_{i,j}^{k+1} + U_{i,j}^k)\right) \\ &+ \frac{(\theta_{i,j}^{k+1} + \theta_{i,j}^k)}{2} - M\frac{(U_{i,j}^{k+1} + U_{i,j}^k)}{2} + \left(\frac{R^*}{R_{\max} - R_0}\right)\frac{\partial}{\partial R}(g_{i,j}^{k+1} + g_{i,j}^k), \end{aligned} \tag{19}$$

$$\begin{aligned} & \frac{(g_{i,j}^{k+1} - g_{i,j}^k)}{\Delta t} + \left(\frac{U_{i,j}^k}{X_{\max}}\right)\frac{\partial}{\partial X}(g_{i,j}^{k+1} + g_{i,j}^k) + \left(\frac{V_{i,j}^k}{R_{\max} - R_0}\right)\frac{\partial}{\partial R}(g_{i,j}^{k+1} + g_{i,j}^k) \\ &= \left(\frac{\sqrt{2\lambda}}{R_{\max} - R_0}\right)^2\frac{\partial^2}{\partial R^2}(g_{i,j}^{k+1} + g_{i,j}^k) + \left(\frac{\lambda}{R_{\max} - R_0}\right)\frac{1}{\bar{R}}\frac{\partial}{\partial R}(g_{i,j}^{k+1} + g_{i,j}^k) \\ &+ R^*B\left(\frac{1}{R_{\max} - R_0}\right)\frac{\partial}{\partial R}(U_{i,j}^{k+1} + U_{i,j}^k) - \left(\frac{R^*B}{R_0^2 X_{\max}}\right)\frac{\partial}{\partial X}(V_{i,j}^{k+1} + V_{i,j}^k) \\ &- R^*B(g_{i,j}^{k+1} + g_{i,j}^k), \end{aligned} \tag{20}$$

$$\begin{aligned} & \frac{(\theta_{i,j}^{k+1} - \theta_{i,j}^k)}{\Delta t} + \left(\frac{U_{i,j}^k}{X_{\max}}\right)\frac{\partial}{\partial X}(\theta_{i,j}^{k+1} + \theta_{i,j}^k) + \left(\frac{V_{i,j}^k}{R_{\max} - R_0}\right)\frac{\partial}{\partial R}(\theta_{i,j}^{k+1} + \theta_{i,j}^k) \\ &= \frac{1}{\text{Pr}}\left(\frac{1 + S\theta}{R_{\max} - R_0}\right)\left(\frac{2}{R_{\max} - R_0}\frac{\partial^2}{\partial R^2}(\theta_{i,j}^{k+1} + \theta_{i,j}^k) + \frac{1}{\bar{R}}\frac{\partial}{\partial R}(\theta_{i,j}^{k+1} + \theta_{i,j}^k)\right) \\ &+ \frac{S}{\text{Pr}}\left(\frac{\sqrt{2}}{R_{\max} - R_0}\right)^2\left(\frac{\partial\theta_{i,j}^k}{\partial R}\right)\frac{\partial}{\partial R}(\theta_{i,j}^{k+1} + \theta_{i,j}^k) - F\left(\frac{(\theta_{i,j}^{k+1} + \theta_{i,j}^k)}{2} - 1\right), \end{aligned} \tag{21}$$

where,

$$\bar{R} = (R + 1)\left(\frac{R_{\max} - R_0}{2}\right) + R_0.$$

Thus, by applying the Chebyshev collocation approximation to the equations (18-21), we obtain the following Chebyshev collocation equations:

$$\left(\frac{1}{\mathbf{X}_{\max}}\right)\left(\sum_{l=0}^{L_1} d_{i,l}^{(1)}U_{l,j}^{k+1} + \sum_{l=0}^{L_1} d_{i,l}^{(1)}U_{l,j}^k\right) + \left(\frac{1}{\mathbf{R}_{\max} - \mathbf{R}_0}\right)\left(\sum_{l=0}^{L_2} \tilde{d}_{j,l}^{(1)}V_{i,l}^{k+1} + \sum_{l=0}^{L_2} \tilde{d}_{j,l}^{(1)}V_{i,l}^k\right) + \frac{V_{i,j}^{k+1}}{R} = 0, \tag{22}$$

$$\begin{aligned} & \frac{(U_{i,j}^{k+1} - U_{i,j}^k)}{\Delta t} + \left(\frac{U_{i,j}^k}{\mathbf{X}_{\max}}\right)\left(\sum_{l=0}^{L_1} d_{i,l}^{(1)}U_{l,j}^{k+1} + \sum_{l=0}^{L_1} d_{i,l}^{(1)}U_{l,j}^k\right) \\ & + \left(\frac{V_{i,j}^k}{\mathbf{R}_{\max} - \mathbf{R}_0}\right)\left(\sum_{l=0}^{L_2} \tilde{d}_{j,l}^{(1)}U_{i,l}^{k+1} + \sum_{l=0}^{L_2} \tilde{d}_{j,l}^{(1)}U_{i,l}^k\right) \\ & = \frac{(\theta_{i,j}^{k+1} + \theta_{i,j}^k)}{2} + 2\left(\frac{1}{\mathbf{R}_{\max} - \mathbf{R}_0}\right)^2\left(\sum_{l=0}^{L_2} \tilde{d}_{j,l}^{(2)}U_{i,l}^{k+1} + \sum_{l=0}^{L_2} \tilde{d}_{j,l}^{(2)}U_{i,l}^k\right) \\ & + \frac{1}{(\mathbf{R}_{\max} - \mathbf{R}_0)\tilde{R}}\left(\sum_{l=0}^{L_1} d_{i,l}^{(1)}U_{l,j}^{k+1} + \sum_{l=0}^{L_1} d_{i,l}^{(1)}U_{l,j}^k\right) - M\frac{(U_{i,j}^{k+1} + U_{i,j}^k)}{2} \\ & + \left(\frac{R^*}{\mathbf{R}_{\max} - \mathbf{R}_0}\right)\left(\sum_{l=0}^{L_2} \tilde{d}_{j,l}^{(1)}g_{i,l}^{k+1} + \sum_{l=0}^{L_2} \tilde{d}_{j,l}^{(1)}g_{i,l}^k\right), \end{aligned} \tag{23}$$

$$\begin{aligned} & \frac{(g_{i,j}^{k+1} - g_{i,j}^k)}{\Delta t} + \left(\frac{U_{i,j}^k}{\mathbf{X}_{\max}}\right)\left(\sum_{l=0}^{L_1} d_{i,l}^{(1)}g_{l,j}^{k+1} + \sum_{l=0}^{L_1} d_{i,l}^{(1)}g_{l,j}^k\right) \\ & + \left(\frac{V_{i,j}^k}{\mathbf{R}_{\max} - \mathbf{R}_0}\right)\left(\sum_{l=0}^{L_2} \tilde{d}_{j,l}^{(1)}g_{i,l}^{k+1} + \sum_{l=0}^{L_2} \tilde{d}_{j,l}^{(1)}g_{i,l}^k\right) \\ & = \left(\frac{\sqrt{2\lambda}}{\mathbf{R}_{\max} - \mathbf{R}_0}\right)^2\left(\sum_{l=0}^{L_2} \tilde{d}_{j,l}^{(2)}g_{i,l}^{k+1} + \sum_{l=0}^{L_2} \tilde{d}_{j,l}^{(2)}g_{i,l}^k\right) \\ & + \left(\frac{\lambda}{\mathbf{R}_{\max} - \mathbf{R}_0}\right)\frac{1}{\tilde{R}}\left(\sum_{l=0}^{L_2} \tilde{d}_{j,l}^{(1)}g_{i,l}^{k+1} + \sum_{l=0}^{L_2} \tilde{d}_{j,l}^{(1)}g_{i,l}^k\right) \\ & + \left(\frac{R^*B}{\mathbf{R}_{\max} - \mathbf{R}_0}\right)\left(\sum_{l=0}^{L_2} \tilde{d}_{j,l}^{(1)}U_{i,l}^{k+1} + \sum_{l=0}^{L_2} \tilde{d}_{j,l}^{(1)}U_{i,l}^k\right) \\ & - \frac{1}{\mathbf{R}_0^2}\left(\frac{R^*B}{\mathbf{X}_{\max}}\right)\left(\sum_{l=0}^{L_1} d_{i,l}^{(1)}V_{l,j}^{k+1} + \sum_{l=0}^{L_1} d_{i,l}^{(1)}V_{l,j}^k\right) - R^*B(g_{i,j}^{k+1} + g_{i,j}^k), \end{aligned} \tag{24}$$

$$\begin{aligned}
 & \frac{(\theta_{i,j}^{k+1} - \theta_{i,j}^k)}{\Delta t} + \left(\frac{U_{i,j}^k}{X_{\max}} \right) \left(\sum_{l=0}^{L_1} d_{i,l}^{(1)} \theta_{l,j}^{k+1} + \sum_{l=0}^{L_1} d_{i,l}^{(1)} \theta_{l,j}^k \right) \\
 & + \left(\frac{V_{i,j}^k}{R_{\max} - R_0} \right) \left(\sum_{l=0}^{L_2} \tilde{d}_{j,l}^{(1)} \theta_{i,l}^{k+1} + \sum_{l=0}^{L_2} \tilde{d}_{j,l}^{(1)} \theta_{i,l}^k \right) \\
 & = \frac{2(1 + S\theta_{i,j}^k)}{\text{Pr}} \left(\frac{1}{R_{\max} - R_0} \right)^2 \left(\sum_{l=0}^{L_2} \tilde{d}_{j,l}^{(2)} \theta_{i,l}^{k+1} + \sum_{l=0}^{L_2} \tilde{d}_{j,l}^{(2)} \theta_{i,l}^k \right) \\
 & + \frac{(1 + S\theta_{i,j}^k)}{\text{Pr}} \left(\frac{1}{\tilde{R}(R_{\max} - R_0)} \right) \left(\sum_{l=0}^{L_2} \tilde{d}_{j,l}^{(1)} \theta_{i,l}^{k+1} + \sum_{l=0}^{L_2} \tilde{d}_{j,l}^{(1)} \theta_{i,l}^k \right) \\
 & + \frac{S}{\text{Pr}} \left(\frac{\sqrt{2}}{R_{\max} - R_0} \right)^2 \left(\sum_{l=0}^{L_2} \tilde{d}_{j,l}^{(1)} \theta_{i,l}^k \right) \left(\sum_{l=0}^{L_2} \tilde{d}_{j,l}^{(1)} \theta_{i,l}^{k+1} + \sum_{l=0}^{L_2} \tilde{d}_{j,l}^{(1)} \theta_{i,l}^k \right) \\
 & - F \left(\frac{(\theta_{i,j}^{k+1} + \theta_{i,j}^k)}{2} - 1 \right)
 \end{aligned} \tag{25}$$

This system contains $(4L_1L_2 - 3L_1)$ equations for the unknown $U_{i,j}^k, g_{i,j}^k, \theta_{i,j}^k$ where $i = 1, \dots, L_1, j = 1, \dots, L_2 - 1$ and $V_{i,j}^k$ where $i = 1, \dots, L_1, j = 1, \dots, L_2$ is solved by Newton method (take $X_{\max} = 1.0, R_{\max} = 3.5, L_1 = 12, L_2 = 15$ and $\Delta t = 0.001$). The computer program of the numerical method was executed in MATHEMATICA 5.2TM running on a PC.

6. Results and Discussion

In this section, a comprehensive numerical parametric study is conducted and the results are reported in terms of graphs. This is done in order to illustrate special features of the solutions. So, the numerical solution was obtained for distributions of the dimensionless velocities $U(X, R, t)$, $g(X, R, t)$ and the dimensionless temperature $\theta(X, R, t)$ as well as the local skin-friction coefficient C_f , wall couple stress coefficient M_w and the local Nusselt number N_u .

To study the behavior of these profiles, curves are drawn for various values of the parameters that describe the flow, *e.g.*, the variable micropolar parameter R^* , the variable thermal conductivity parameter S , the magnetic parameter M , the radiation parameter F and the power-law exponent of variable surface temperature m . This values of studied parameters (which took from Ganesan and Rani (2000)) are shown in the Table (1) and the Figs. 2-15. To assess the accuracy of numerical results, the present study is compared with previous study.

No analysis seems to have been presented for the effect of variable thermal conductivity on micropolar fluid flow over vertical cylinder with variable surface temperature. A comparison between the curves of the velocity and the temperature values computed by Ganesan and Rani

(2000) for steady state and their corresponding numerical results for values of $x = 1$, $Pr = 0.7$, $m = 0.2$, ($M = F = S = R^* = B = \lambda = 0$) at $t = 4.0$ is given in Fig. 2. As is evident from this figure the agreement between these results is excellent. This comparison lends confidence in the numerical solutions and shows that the numerical method is adequate for the solution of the present problem.

The variation of the velocity, the angular velocity and temperature profiles with time are shown in Figures (3-5) for various values of t , respectively at $x = 1$, $Pr = 0.7$, $M = 10$, $F = 0.01$, $S = 0.5$, $R^* = 5$, $m = 0.2$, $B = 0.0001$, $\lambda = 0.001$ and $t = 4.5$. It is predicated that after a certain lapse of time, the velocity, the angular velocity and temperature reach steady state. It is also observed that transient profiles of the velocity u decreases in the flow direction but the angular velocity g is maximum near the upstream. The thermal boundary layer thickness and the surface temperature of the cylinder increase in the flow direction.

Fig. 6 show the effect of radiation parameter F on the temperature θ profiles. These calculations have been carried out for values of the radiation parameter $F = 0.01, 0.1, 0.3, 0.5$ and for the time $t = 4.5$ (steady state), it is observed that with increasing the radiation parameter F the temperature increases. This result qualitatively agrees with expectations, since the effect of radiation and surface temperature is to increase the rate of energy transport to the fluid and accordingly increases the temperature of the fluid.

Figures 7 and 8 show that, the velocity and the angular velocity decrease with increasing the parameter M . On the other words, the Lorentz force, which opposes the flow, increases with increasing the magnetic parameter M and leads to enchanced deceleration of the flow, this conclusion meets the logic of the magnetic field exerts a retarding force on the free convection flow. Figures 9 and 10 show that, all of profiles of the velocity and temperature increase with increasing the micropolar parameter R^* .

Fig. 11 shows that, the angular velocity decrease with increasing the micropolar parameter R^* . Fig. 12 display result for the dimensionless temperature θ distribution in the case of steady state ($t = 4.5$) with the variable thermal conductivity. As shown, with increasing the variable thermal conductivity parameter S the temperature increases, where the positive values of S mean that the thermal conductivity k_f increases with an increase in temperature and this is the case for fluid such as water and air, while for negative values of S the thermal conductivity k_f decreases with an increase in temperature and this is the case for fluid such as lubrication oils, where (for air $0 \leq S \leq 6$, for water $0 \leq S \leq 0.12$ and for lubrication oils $-0.1 \leq S \leq 0$) (Schlichting (1972)). Figures 13 and 14 show that, all of profiles of the velocity, the angular velocity decrease with increasing m .

Fig. 15 show that, when m increases the temperature gradient along the cylinder near the leading edge decrease, that is, the impulsive force along the cylinder decreases with increasing m . Figures 8, 11 and 14 show that, the profiles of the angular velocity changes its shape from nearer to the boundary-layer than free-stream of it. By using Eqs. (15-17), the effects of variable micropolar parameter R^* , thermal conductivity parameters S , the radiation parameter F , the

magnetic parameter M and the parameter of surface temperature m on the local skin friction C_f , the local Nusselt number N_u and the wall couple stress coefficient are given in table (1). Table (1) represents the values of C_f , N_u and M_w for various values of the parameter R^* , S , F , M and m at ($x = 1$, $Pr = 0.7$, $B = 0.0001$, $\lambda = 0.001$) and $t = 4.5$ (steady state). It is clear that, C_f , decreases as R^* , S and F increase, whereas C_f , increases as M and m increase. Also, N_u increases as R^* , S , F and M increase, however, N_u decreases as m increases. Finally, M_w decreases as R^* , S and F increase. M_w increase as M and m increase.

7. Conclusions

Chebyshev collocation method is used to compute the effect of variable thermal conductivity on unsteady free-convection in a micro-polar fluid past a semi-infinite vertical cylinder with variable surface temperature in the presence of magnetic field and radiation. Boundary layer and Boussinesq approximations have been introduced together to describe the flow field. The domain of the problem is discretized according to Chebyshev collocation scheme. In this study, the boundary layer equations are transformed into a linear algebraic system by using Chebyshev collocation method in spatial and Crank-Nicolson method in time.

The effects of different physical values of the dimensionless parameters that describe the flow like the variable micropolar parameter, the variable thermal conductivity parameter, the radiation parameter, the magnetic field parameter and the surface temperature parameter on the flow and heat transfer have been discussed. Numerical calculations are carried out for the various parameters used in the MHD convection problem. It is found that as time approaches infinity, the values of the velocity, the temperature and the angular velocity approach to the steady state values. The velocity distribution increases as micropolar parameter increases but the angular velocity distribution decreases with increasing micropolar parameter while the velocity and the angular velocity distributions decrease as the magnetic parameter and the surface temperature parameter increase.

The temperature distribution increases as the micropolar parameter, the thermal conductivity parameter, the radiation parameter increase, but it decreases as the surface temperature parameter increases. Moreover, the friction factor C_f decreases as R^* , S and F increase, whereas it increases as M and m increase. Also, the local Nusselt number N_u increases as R^* , S , F and M increase, however, it decreases as m increases. The wall couple stress coefficient M_w decreases as R^* , S and F increase, but it increase as M and m increase. Finally, taking into account the variation of the fluid properties especially the thermal conductivity with temperature and using the same analysis used in this work can improve many results obtained before, for example Ganesan and Rani (2000). It is hoped that the present work will serve as a vehicle for understanding more complex problems involving the various physical effects investigated in the present problem.

REFERENCES

- Badr, H. M. and Dennis, S. C. R. (1985). The Time Dependent Viscous Flow past an Impulsively Started Rotating and Translating Circular Cylinder. *Journal of Fluid Mech.*, Vol. 158, pp. 447-488.
- Cheng, P. C. and Huann, M. C. (1994). Transient Analysis of Natural Convection along a Vertical Wavy Surface in Micropolar Fluids. *International Journal of Engin. Sci.*, Vol. 32 (1), pp. 19-33.
- Cogley, A. C., Vincenti, W. G. and Gilles, S. E. (1968). Differential Approximation for Radiation Transfer in a Non-Gray Near Equilibrium, *AIAA Journal*, Vol. 6, pp. 551.
- Chen, T. S. and Yih, C. F. (1980). Combined Heat and Mass Transfer in Natural Convection along Vertical Cylinder. *International Journal of Heat and Mass Transfer*, Vol. 23, pp. 451-461.
- Collins, W. M. and Dennis, S. C. R. (1973). Flow past an Impulsively Started Circular Cylinder. *Journal of Fluid Mech*, Vol. 60, pp. 105-127.
- Dring, R. P. and Gebhart, B. (1966). Transient Natural Convection from Thin Vertical Cylinders. *Journal of Heat Transfer*, Vol. 88, pp. 246-247.
- Elbarbary, E. M. E. and El-Sayed, M. S. (2005). Higher Order Pseudospectral Differentiation Matrices. *Appl. Numerical Math.*, Vol. 55, pp. 425-438.
- Elbarbary, E. M. E. and El-Kady, M. (2003). Chebyshev Finite-Difference Approximation for the Boundary Value Problems. *Applied Math. and Computations*, Vol. 139, pp. 513-523.
- Elgazery, N. S. (2008). An Implicit-Chebyshev Pseudospectral Method for the Effect of Radiation on Power-law Fluid past a Vertical Plate Immersed in a Porous Medium. *Communications in Nonlinear Science and Numerical Simulation*, Vol. 13, pp. 728-744.
- Erigen, A. C. (1966). Theory of Micropolar Fluids, *Journal of Math. Mech*, Vol. 16, pp. 1-18.
- Erigen, A. C. (1972). Theory of Thermomicro-polar Fluids. *Journal of Math. Anal. Appl*, Vol. 38, pp. 480-496.
- Evans, L. B., Reid, T. C. and Drake, E. M. (1980). Transient Natural Convection in Vertical Cylinder. *AIChE Journal*, Vol. 14, pp. 251-256.
- Lee, H. R., Chen, T. S. and Armaly (1988). Natural Convection along Slender Vertical Cylinders with Variable Surface Temperature. *Journal of Heat Transfer*, Vol. 110, pp. 103-108.
- Ganesan, P. and Rani, H. P. (1998). Transient Natural Convection along Vertical Cylinder with Heat and Mass Transfer. *Heat and Mass Transfer*, Vol. 33, pp. 449-455.
- Ganesan, P. and Rani, H. P. (2000). Transient Natural Convection Flow over Vertical Cylinder with Variable Surface Temperatures. *Forschung im Ingenieurwesen*, Vol. 66, pp.11-16.
- Ganesan, P. and Loganathan, P. (2001). Transient Free Convection Flow past an Impulsively Started Isothermal Vertical Cylinder with Mass Flux. *Forschung im Ingenieurwesen*, Vol. 66, pp. 235-240.
- Ganesan, P. and Loganathan, P. (2001). Effects of Mass Transfer and Flow past a Moving Vertical Cylinder with Constant Heat Flux. *Acta Mechanica*, Vol. 150, pp. 179-190.
- Ganesan, P. and Loganathan, P. (2001). Unsteady Natural Convection Flow past a Moving Vertical Cylinder with Heat and Mass Transfer. *Heat and Mass Transfer*, Vol. 37, pp. 59-65.
- Ganesan, P. and Loganathan, P. (2002). Heat and Mass Flux Effects on a Moving Vertical Cylinder with Chemically Reactive Species Diffusion. *Journal of Engineering Physics and Thermophysics*, Vol. 75, pp. 105-114.
- Ganesan, P. and Loganathan, P. (2003). Magnetic Field Effect on a Moving Vertical Cylinder with Constant Heat Flux. *Heat and Mass Transfer*, Vol. 39, pp. 381-386.

Ganesan, P. and Loganathan, P. (2006). Numerical Study of Double-Diffusive, Free Convective Flow past a Moving Vertical Cylinder. *Journal of Engineering Physics and Thermophysics*, Vol. 79 (1), pp. 73-78.

Schlichting, H. D. C. (1972). *Boundary-layer theory*, Mc Graw-Hill, New York.

Velusamy, K. and Garg, V. K. (1992). Transient Natural Convection over a Heat Generating Vertical Cylinder. *International Journal of Heat and Mass Transfer*, Vol. 35, pp.1293-1306.

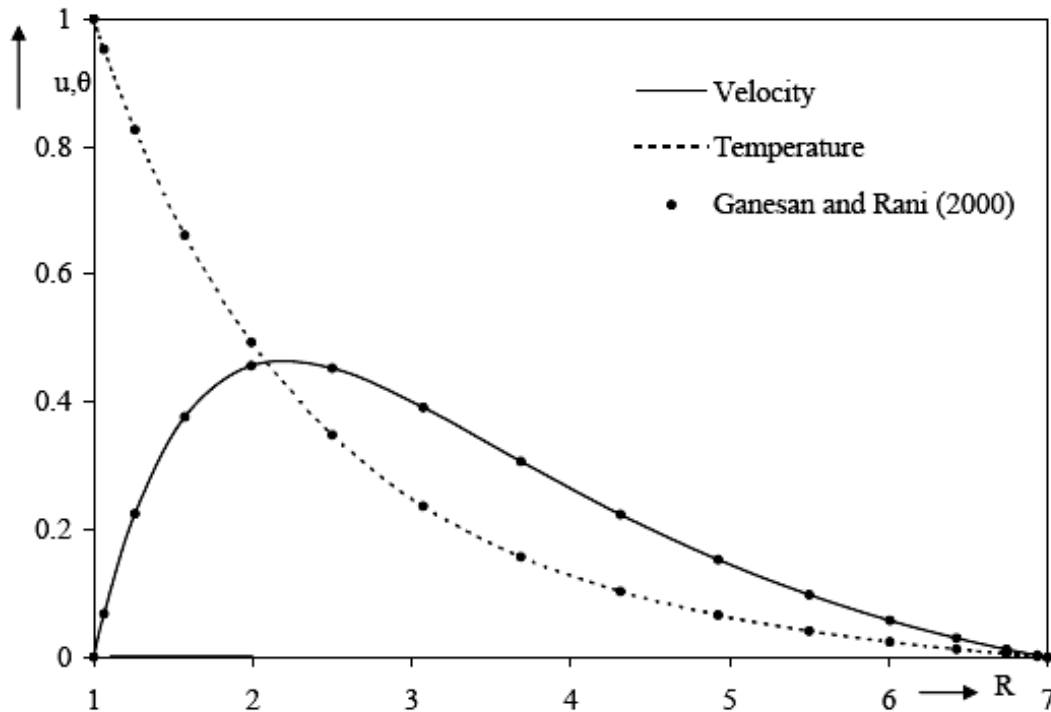


Fig.2. Comparison of Temperature profiles with Ganesan and Rani (2000) at $t=4.0, x=1, Pr=0.7, F=0, S=0, M=0, R^*=0, m=0.2, B=0, \lambda=0$

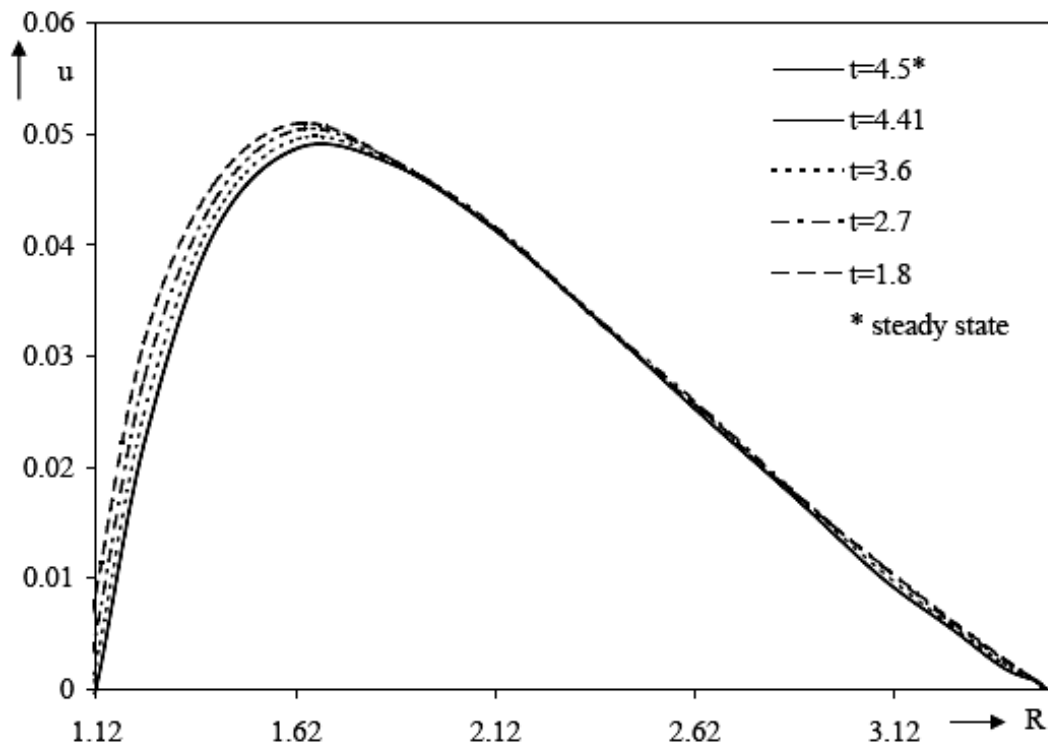


Fig.3. Steady state of velocity profiles at $x=1, Pr=0.7, F=0.01, S=0.5, M=10, R^*=5, m=0.2, \lambda = 0.001, B = 0.0001$

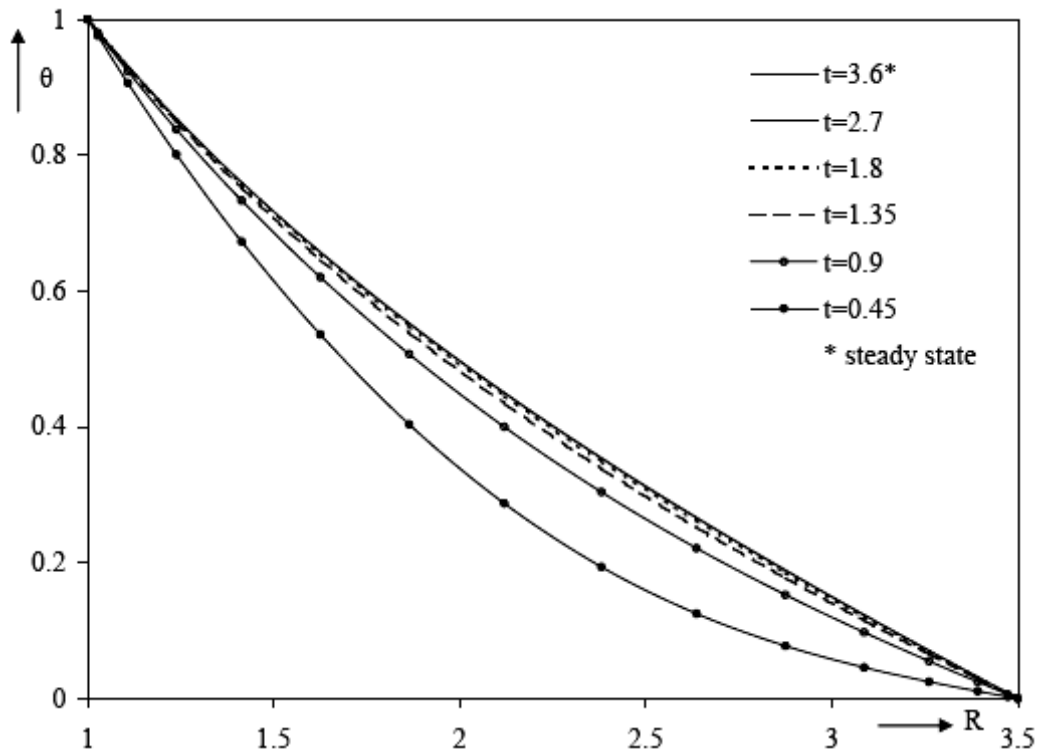


Fig.4. Steady state of temperature profiles at $x=1$, $Pr=0.7$, $F=0.01$, $S=0.5$, $M=10$, $R^*=5$, $m=0.2$, $\lambda = 0.001$, $B = 0.0001$

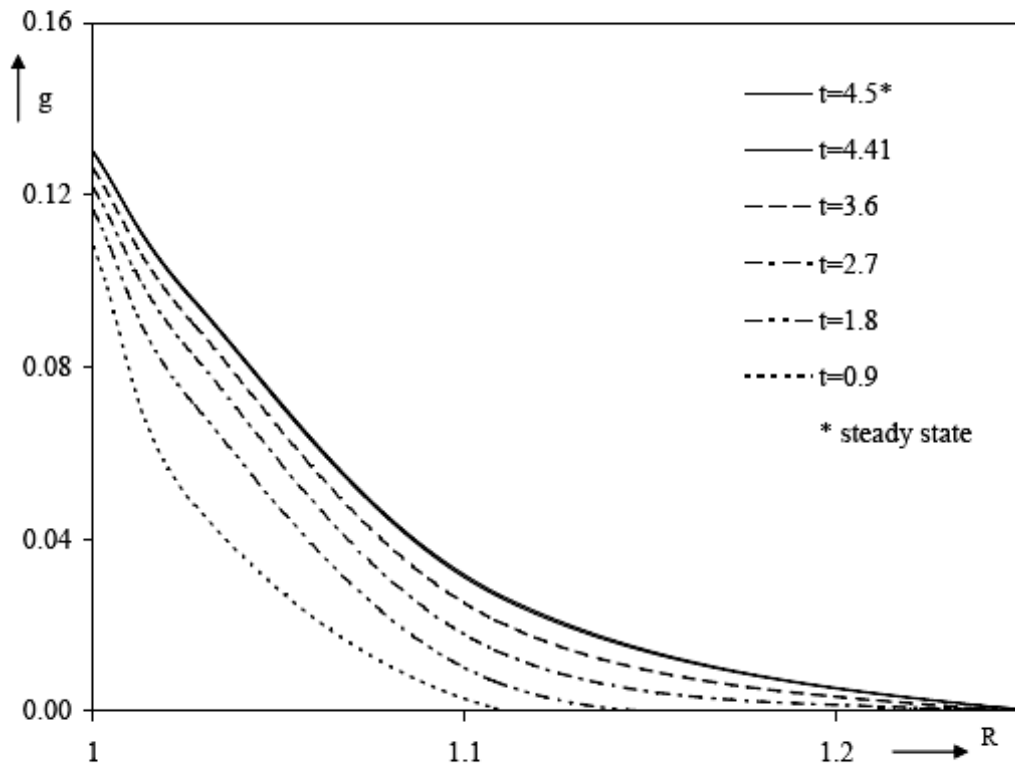


Fig.5. Steady state of angular velocity profiles at $x=1$, $Pr=0.7$, $F=0.01$, $S=0.5$, $M=10$, $R^*=5$, $m=0.2$, $\lambda = 0.001$, $B = 0.0001$

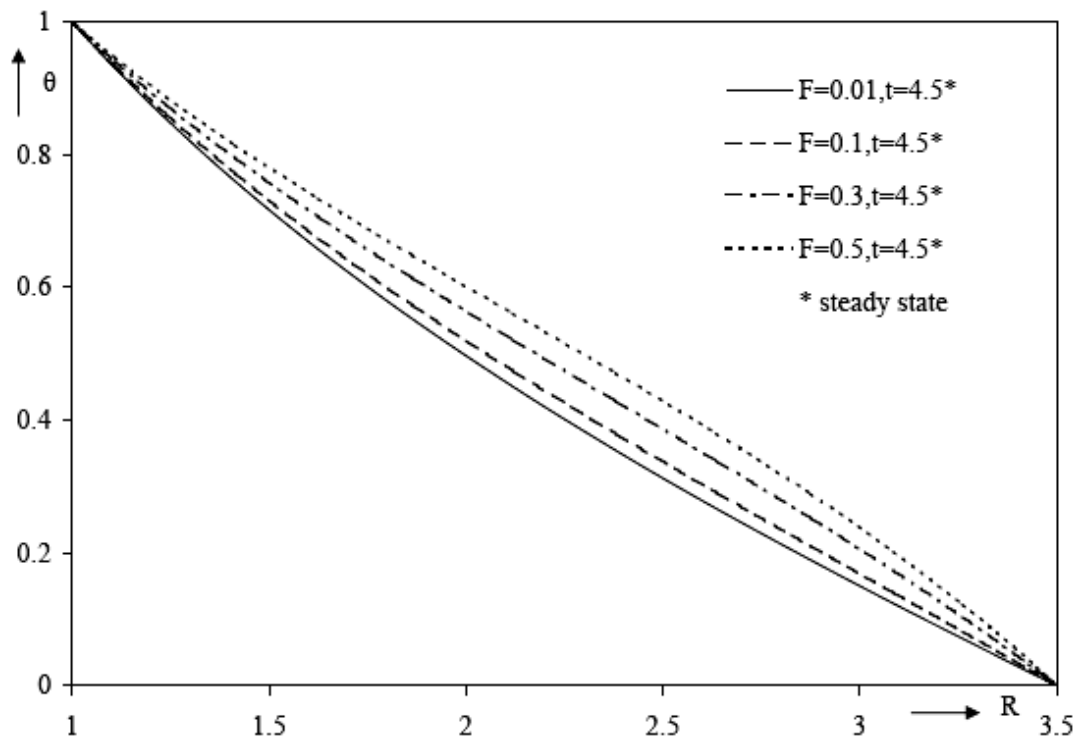


Fig.6. Transient temperature profiles for the different values of parameter F at $x=1$, $Pr=0.7$, $S=0.5$, $M=10$, $R^*=5$, $m=0.2$, $\lambda = 0.001$, $B = 0.0001$

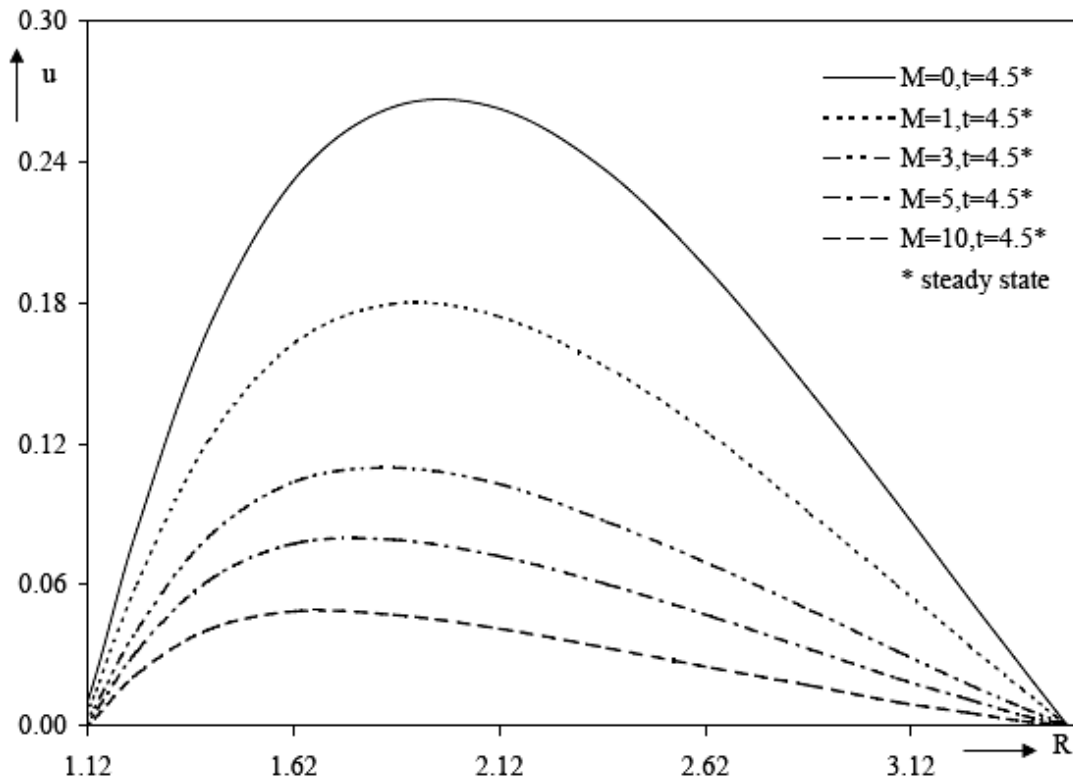


Fig.7. Transient velocity profiles for the different values of parameter M at $x=1$, $Pr=0.7$, $S=0.5$, $F=0.01$, $R^*=5$, $m=0.2$, $\lambda = 0.001$, $B = 0.0001$

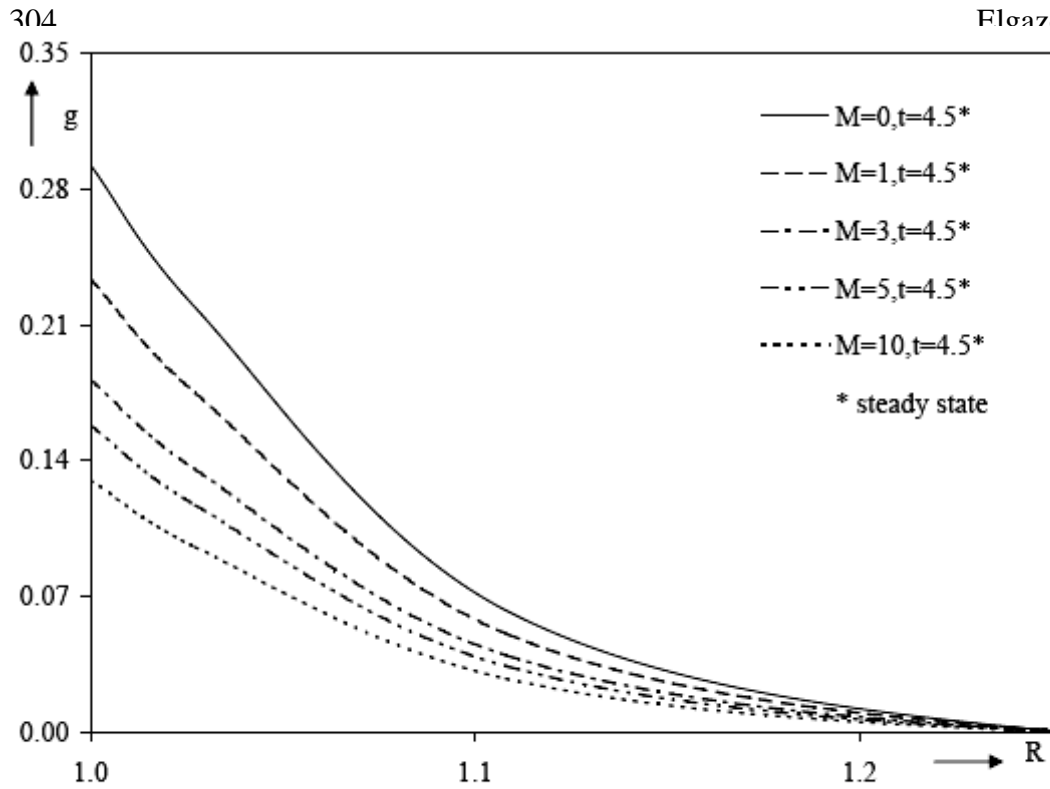


Fig.8. Transient angular velocity profiles for the different values of parameter M at $x=1$, $Pr=0.7$, $S=0.5$, $F=0.01$, $R^*=5$, $m=0.2$, $\lambda = 0.001$, $B = 0.0001$

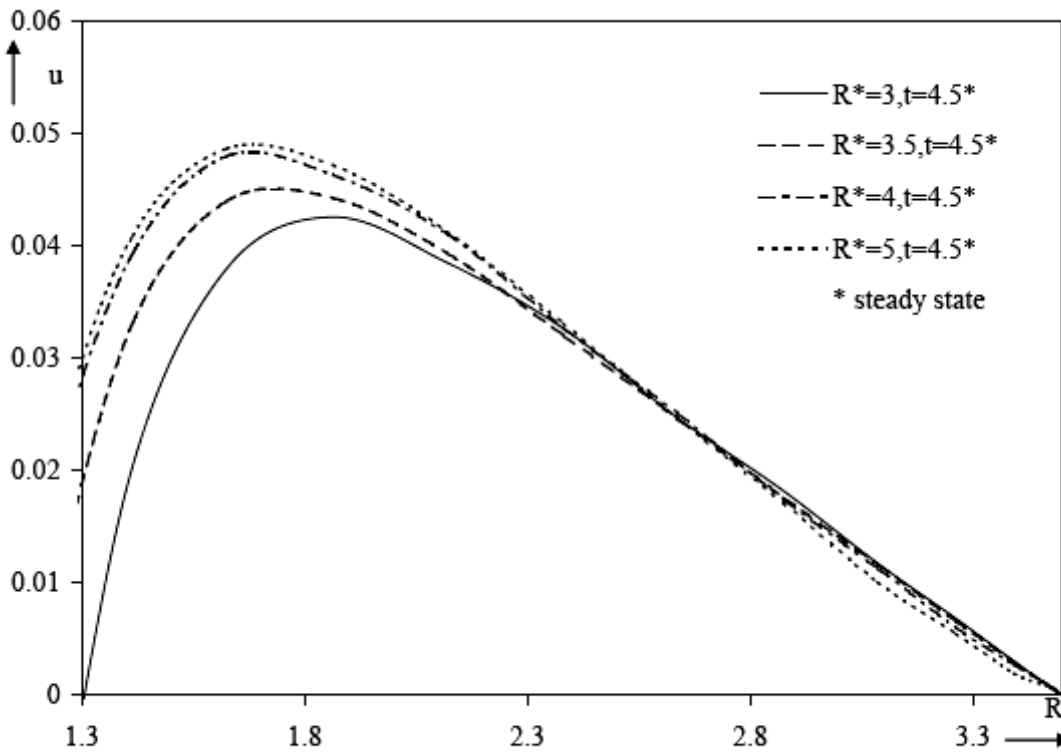


Fig.9. Transient velocity profiles for the different values of parameter R^* at $x=1$, $Pr=0.7$, $S=0.5$, $M=10$, $F=0.01$, $m=0.2$, $\lambda = 0.001$, $B = 0.0001$

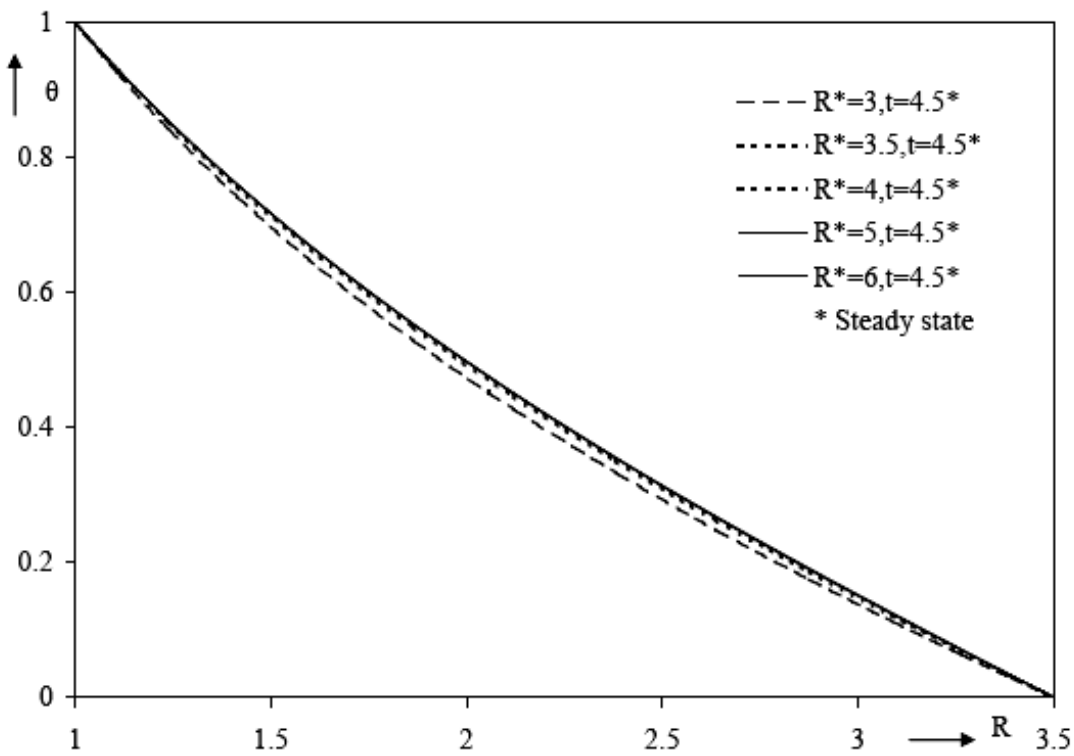


Fig.10. Transient temperature profiles for the different values of parameter R^* at $x=1, Pr=0.7, S=0.5, M=10, F=0.01, m=0.2, \lambda = 0.001, B = 0.0001$

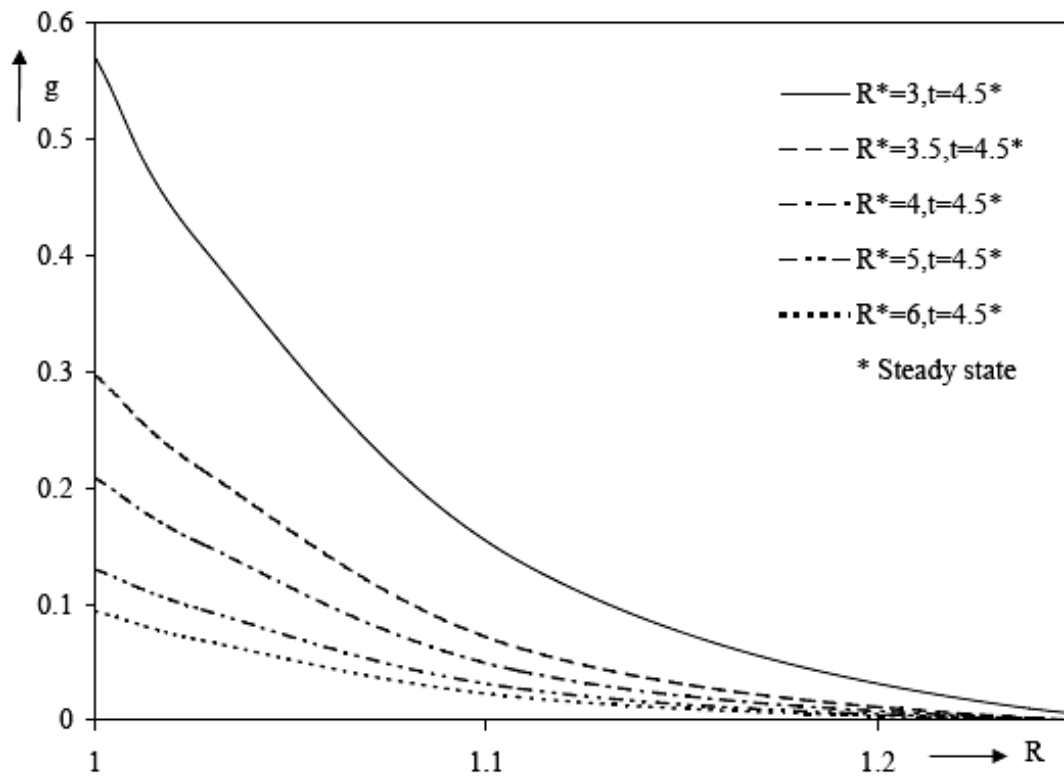


Fig.11. Transient angular velocity profiles for the different values of parameter R^* at $x=1, Pr=0.7, S=0.5, M=10, F=0.01, m=0.2, \lambda = 0.001, B = 0.0001$

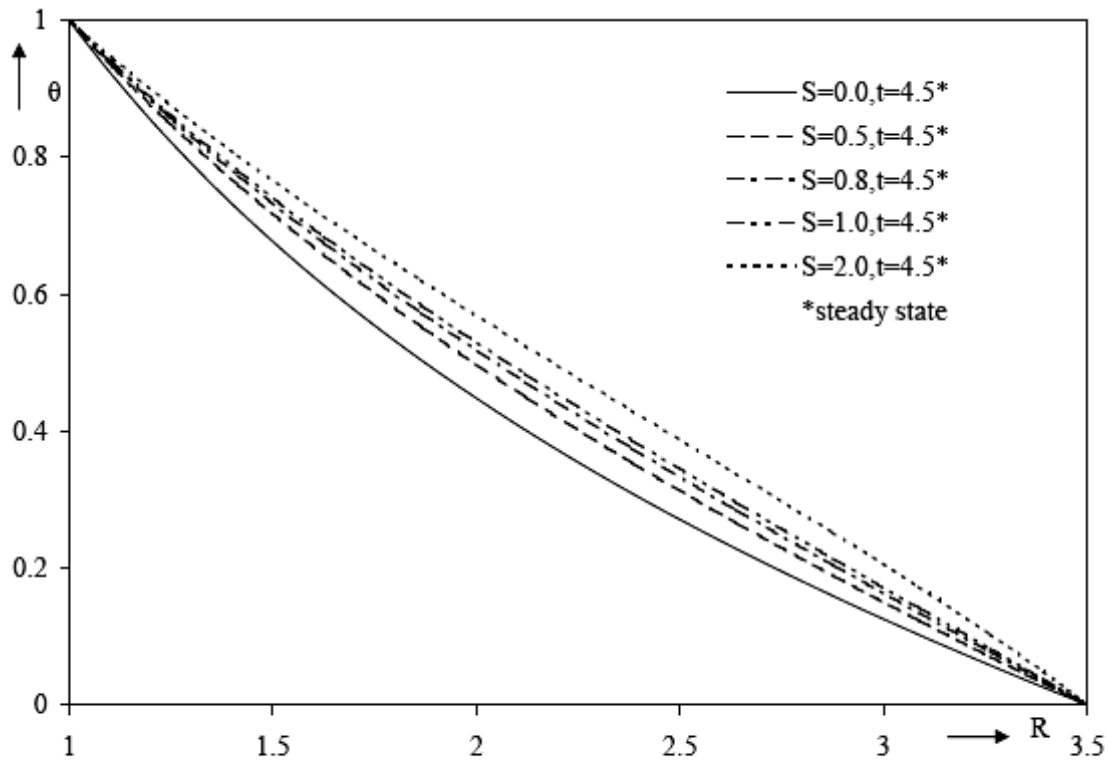


Fig.12. Transient temperature profiles for the different values of parameter S at $x=1$, $Pr=0.7$, $M=10$, $F=0.01$, $R^*=5$, $m=0.2$, $\lambda = 0.001$, $B = 0.0001$

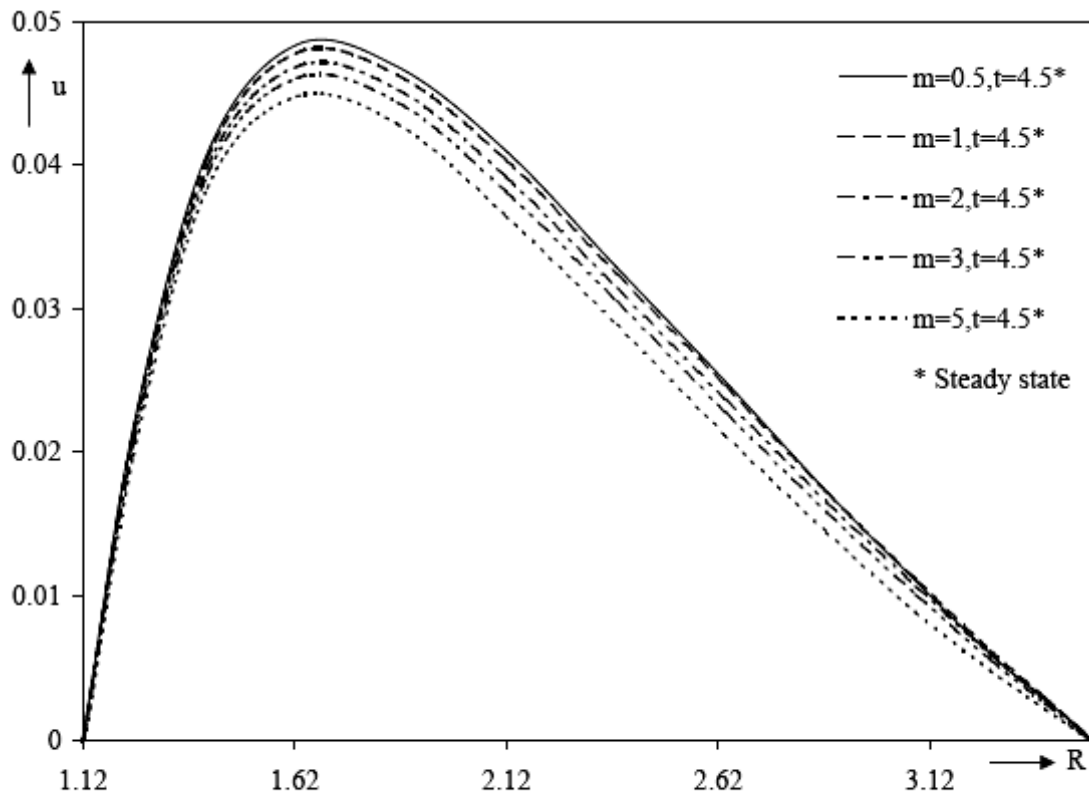


Fig.13. Transient velocity profiles for the different values of parameter m at $x=1$, $Pr=0.7$, $S=0.5$, $M=10$, $F=0.01$, $R^*=5$, $\lambda = 0.001$, $B = 0.0001$

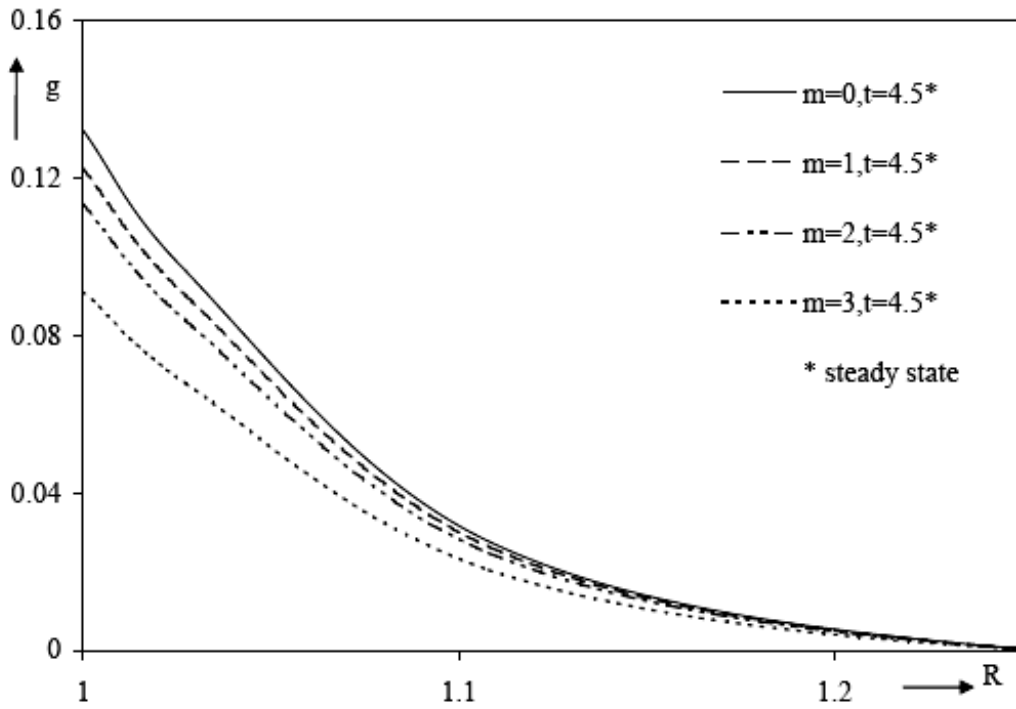


Fig.14. Transient angular velocity profiles for the different values of parameter m at $x=1$, $Pr=0.7$, $S=0.5$, $M=10$, $F=0.01$, $R^*=5$, $m=0.2$, $\lambda = 0.001$, $B = 0.0001$

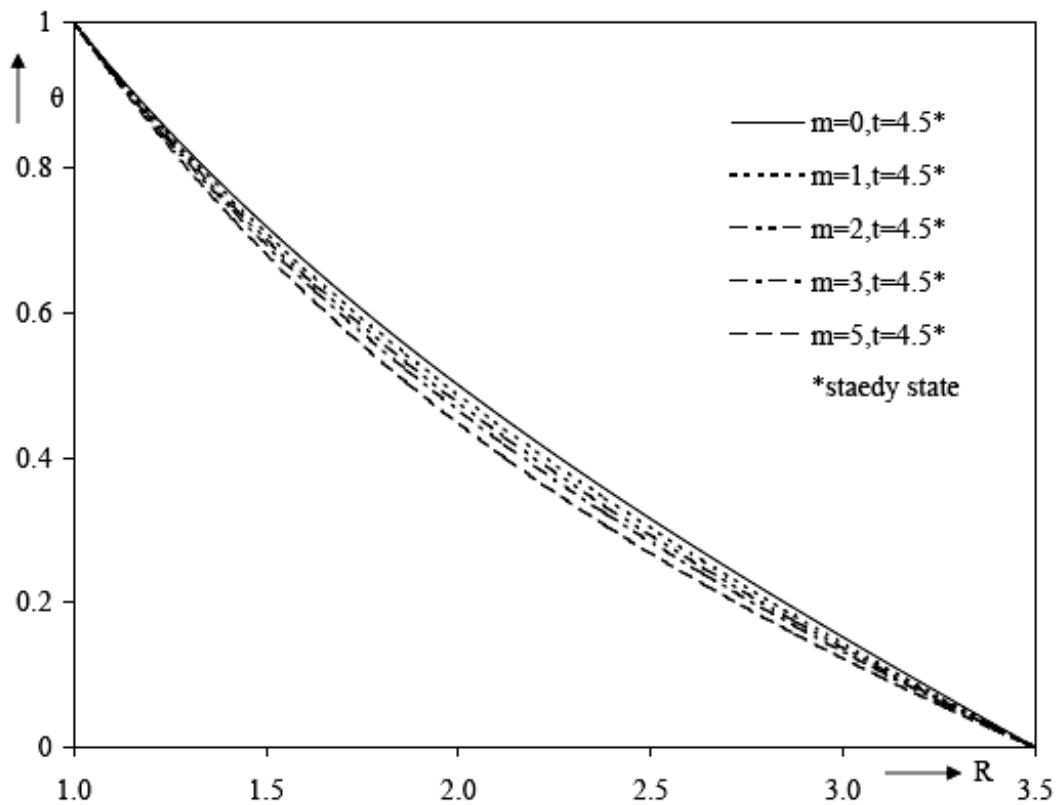


Fig.15. Transient temperature profiles for the different values of parameter m at $x=1$, $Pr=0.7$, $S=0.5$, $M=10$, $F=0.01$, $R^*=5$, $\lambda = 0.001$, $B = 0.0001$